

# Layered Tetrahedral Meshing of Thin-Walled Solids for Plastic Injection Molding FEM

Soji Yamakawa  
soji@andrew.cmu.edu

Charles Shaw  
cshaw@cmu.edu

Kenji Shimada  
shimada@cmu.edu

The Department of Mechanical Engineering,  
Carnegie Mellon University,  
5000 Forbes Ave.,  
Pittsburgh, PA 15213

## Abstract

This paper describes a method for creating a well-shaped, layered tetrahedral mesh of a thin-walled solid by adapting the surface triangle sizes to the estimated wall thickness. The primary target application of the method is the finite element analysis of plastic injection molding, in which a layered mesh improves the accuracy of the solution. The edge lengths of the surface triangles must be proportional to the thickness of the domain to create well-shaped tetrahedrons; when the edge lengths are too short or too long, the shape of the tetrahedron tends to become thin or flat. The proposed method creates such a layered tetrahedral mesh in three steps: (1) create a preliminary tetrahedral mesh of the target geometric domain and estimate thickness distribution over the domain; (2) create a non-uniform surface triangular mesh with edge length adapted to the estimated thickness, then create a single-layer tetrahedral mesh using the surface triangular mesh; and (3) subdivide tetrahedrons of the single-layer mesh into multiple layers by applying a subdivision template. The effectiveness of the layered tetrahedral mesh is verified by running some experimental finite element analyses of plastic injection molding.

**Keywords:** Tetrahedral mesh, Plastic injection molding, Finite element method

**Categories:** I.3.5 [Computer Graphics]: Computational Geometry and Object Modeling – Geometric Algorithms, Languages, and Systems; J.6 [Computer Applications]: Computer-Aided Engineering – Computer-Aided Design

## 1 Introduction

The paper describes a method for creating a layered tetrahedral mesh of a thin-walled solid such as cell-phone cases, or a laptop shell cases, which are created by injection molding. A solid is a thin-walled solid when it can be approximated well by a shell structure. For example, most sheet metal parts and injection-molded plastic parts are thin-walled solids. A layered mesh is a mesh in which the number of layers of elements is uniform over the mesh. In this paper, we define the number of layers as the smallest number of edges that need to be traversed from a node on one surface of the thin-wall to a node on the other side. Such

number becomes ambiguous for the nodes located on a sidewall or at an intersection of walls. However, if a solid is a thin-walled solid, only a small number of nodes possess such ambiguity. Injection molding is a manufacturing process of injecting high-pressure molten plastic resin into a mold. Parts are then allowed to cool briefly and removed. This process is used for manufacturing a variety of plastic parts such as cell phone cases, laptop shells and other consumer electronics.

The proposed method creates well-shaped tetrahedral elements by controlling the sizes of the surface triangles based on the estimated thickness. When a surface triangle is small compared to the thickness of the target geometric domain, the tetrahedron created from the triangle becomes sharp as shown in Figure 1 (a), or when the triangle is large, the tetrahedron becomes flat as shown in Figure 1 (b); the size of the surface triangle thus must be appropriate for the thickness to have a well-shaped element as shown in Figure 1 (c). Since the thickness can vary over the domain, the surface triangular mesh must be a non-uniform mesh with element size based on the thickness distribution. To make such a surface triangular mesh and well-shaped tetrahedral elements, the proposed method first creates a preliminary tetrahedral mesh of the target geometric domain with no interior node from a fine surface triangular mesh, and then estimates the thickness distribution. The proposed method then creates a non-uniform surface triangular mesh with element size controlled based on the thickness distribution, and a single-layer output tetrahedral mesh is created from the surface triangular mesh without inserting interior nodes. Finally the elements in the single-layer mesh are subdivided into layers by applying a subdivision template.

The main application of the proposed method is plastic injection molding simulation, via finite element method where high quality layered tetrahedral mesh is particularly useful for obtaining good results. In fact, series of finite element analyses conducted in this research indicate that increasing the number of layers improves the accuracy of the solution more effectively than increasing the resolution of the mesh uniformly.

Using an anisotropic mesh adapted for the analysis result may improve the result. However, plastic injection molding simulation consists of two parts -- mold flow simulation and warpage analysis, and a mesh adapted for the gradient of one of the analyses results may not be suitable for the other analysis. We believe that a high-quality layered mesh is the best compromise for both mold flow simulation and warpage analysis.

The proposed method takes a target geometric domain of a thin-walled solid and the number of layers as input and creates a

layered tetrahedral mesh in three steps: (1) create a preliminary tetrahedral mesh with no interior nodes from a fine surface triangular mesh and estimate the thickness distribution over the surface of the target geometric domain using the preliminary tetrahedral mesh, (2) create a non-uniform surface triangular mesh with element size proportional to the estimated thickness and create a single-layer tetrahedral mesh from the surface triangular mesh, and (3) subdivide tetrahedrons included in the single-layer mesh into layers by applying a subdivision template. The element size of the surface triangular mesh created in the second step is controlled so that the edge length becomes proportional to the estimated thickness. The proposed method controls anisotropy of the output mesh by changing the ratio between the edge length of the surface triangular mesh and the estimated thickness. If the ratio is  $1:\sqrt{2/3}$ , most tetrahedrons become close to an equilateral tetrahedron; the output tetrahedral mesh becomes an isotropic mesh. However, an anisotropic mesh with elements stretched along the surface is often more suitable for injection molding simulation, and for such purposes, the proposed method uses a different ratio such as  $1.5:\sqrt{2/3}$  to create an anisotropic mesh. More detailed discussion on the ratio and the anisotropy is found in Section 4.

A series of finite element analyses have been performed in this research with layered meshes created by the proposed method. The results indicate that having more layers is more effective in improving the solution accuracy than uniformly increasing the mesh resolution. Furthermore, the results show that a layered anisotropic mesh with tetrahedral elements stretched along the boundary gives nearly as accurate result as an isotropic mesh. Hence, with such an anisotropic layered mesh, an accurate solution can be obtained without significantly increasing the number of elements.

The organization of the paper is as follows: Section 2 reviews some existing researches on adaptive mesh generation. Sections 3, 4, and 5 explain the three major steps of the proposed method respectively, thickness estimation, single-layer tetrahedral mesh generation, and subdivision of the single-layer tetrahedral mesh into  $n$  layers. Section 6 discusses some limitations of the proposed method. Some examples of layered meshes are shown in Section 7. Section 8 shows results of finite element analysis of plastic injection molding using the meshes created by the proposed method. Section 9 concludes the paper.

## 2 Related Work

Adaptive mesh generation techniques have been developed mainly for adapting the mesh for the solution of the finite element analysis [Castro-Diaz et al. 1995; Frey and Alauzet 2003; Habashi et al. 1998; Peraire et al. 1988; Peraire et al. 1992; Peraire et al. 1987; Zienkiewicz and Zhu 1991]. These methods first obtain a solution result by running a preliminary finite element analysis with a uniform mesh, and then modify the mesh so that the analysis with the new mesh results in more accurate solution.

Quadros and Shimada present a method for creating a layered all-hex mesh on thin section solids [Quadros and Shimada 2002]. This method creates a tetrahedral mesh of the target geometric domain and extracts an approximation of the medial surface, called a chordal surface, from the tetrahedral mesh. It then produces a quadrilateral mesh of the chordal surface, and hexahedral elements are created by extruding the quadrilateral mesh in the thickness direction. Although this method tends to

yield well-shaped hexahedral elements, it cannot deal with complex geometry where the chordal surface has complex intersections.

Several research efforts are based on mesh sizing and anisotropy control using the geometric feature. A typical approach is to adapt a mesh to the curvature of a target geometry [Shimada et al. 2000; Surazhsky et al. 2003]. These methods control element size or anisotropy so that smaller elements are created in a region where the surface curvature is high. A method for controlling element sizes based on the quadric error metric is presented in [Garland and Heckbert 1997]. This method applies an edge collapse transformation where the transformation does not violate a prescribed error threshold. A method that creates boundary-aligned tetrahedral mesh is presented in [Garimella and Shephard 2000]. This method creates layers of tetrahedral elements nearby the boundary surface; the rest of the target volume is filled using an octree-based mesh generation scheme.

Some methods for building an element sizing function from a target geometric domain are also presented [Persson 2004; Quadros et al. 2004]. These methods inspect the target geometric domain and create a mesh sizing function that gives an appropriate element size in the target domain for approximating the target geometric domain accurately without creating excessively large numbers of elements. A method for interpolating element sizes defined at the nodes of a tetrahedral mesh enclosing the target geometric domain is presented in [Owen and Saigal 2000].

Although the proposed method also creates a sizing function from a target geometric domain, the goal and the approach of the proposed method are different. The goal of the proposed method is to create a layered tetrahedral mesh with well-shaped tetrahedrons, and the sizing function is calculated from the preliminary tetrahedral mesh. And, none of the existing technique creates a clean-layered mesh.

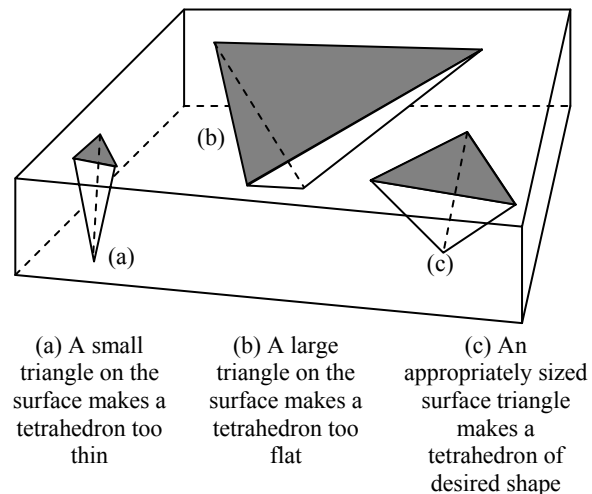


Figure 1 Effect of the size of the surface triangle on the shape of the tetrahedron

### 3 Estimating Thickness of Thin-Walled Solids

The first step of the proposed method creates a preliminary tetrahedral mesh and estimates thickness distribution over the surface of the target geometric domain. The thickness distribution is a function of position and is written as  $t(\mathbf{x})$  where  $\mathbf{x}$  is a position on the surface of the target geometric domain. The purpose of estimating the thickness distribution is to calculate the ideal size of triangles that form a well-shaped tetrahedron when connected to a node lying on the opposite surface.

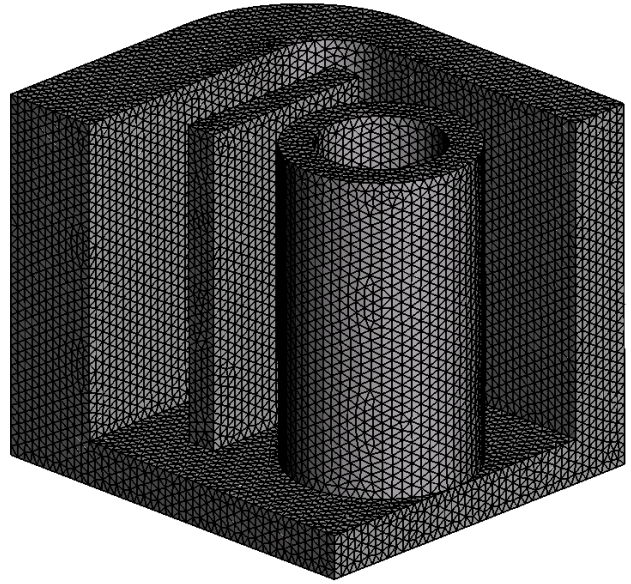
Alternately, thickness may also be estimated without using a preliminary tetrahedral mesh. For example, thickness at a point on the surface can be estimated by shooting a ray from the point in the direction opposite to the surface normal, and taking the length of the ray needed to hit another surface for the first time. However, such a method must handle many exceptions where a unique surface normal cannot be defined, such as corners, where the ray misses the opposite face, hits a wrong face, and etc. As a result, this method may not give the appropriate thickness estimation. On the other hand, a preliminary tetrahedral mesh can be created efficiently, and thickness can be estimated more dependably.

The preliminary tetrahedral mesh is created from a uniform surface triangular mesh that is sufficiently fine for capturing the features of the target geometric domain. The constrained Delaunay tetrahedralization technique [George 1999; George et al. 1991; Shewchuk 2002] creates the preliminary tetrahedral mesh from the surface triangular mesh. No interior nodes are inserted during the process. Figure 2 shows an example of the preliminary tetrahedral mesh.

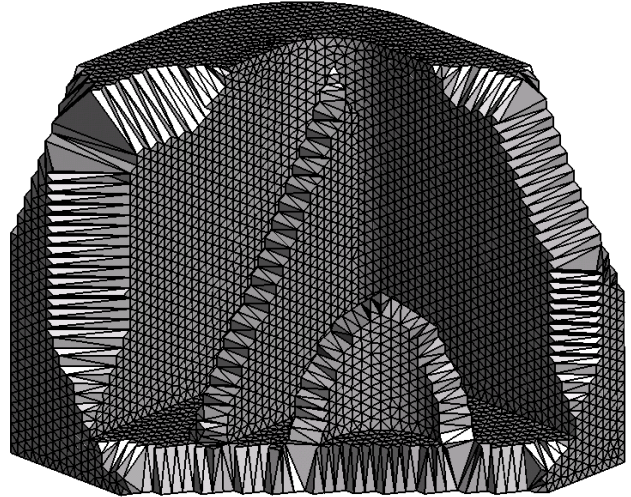
The preliminary tetrahedral mesh includes many needle-like tetrahedrons as shown in Figure 2 (b) because it does not have an interior node, and the density of the surface triangular mesh is high. Many of such needle-like tetrahedrons have only one face exposed to the outside of the mesh as shown in Figure 3. When the exposed face is lying on surface A and the opposite node on surface B, the distance between the exposed face and the opposite node can approximate the thickness if surfaces A and B are opposite such as tetrahedron  $T_1$  shown in Figure 3 (a). However, the distance between the exposed face and the opposite node does not approximate the thickness if the exposed face and the opposite node are lying on non-opposing surfaces in the case of tetrahedron  $T_2$  shown in Figure 3 (a), or if the exposed face and the opposite node are lying on the same surface in the case of tetrahedron  $T_3$  shown in Figure 3 (a). The proposed method thus applies two criteria to identify tetrahedrons that can be used for approximating the thickness:

When a tetrahedron has only one exposed face  $F_x$  and the opposite node of  $F_x$  is  $\mathbf{p}_x$ , the distance between  $F_x$  and  $\mathbf{p}_x$  is an approximated thickness if:

- (1)  $\mathbf{p}_x$  lies within the smallest cylinder that encloses the exposed face whose axial direction is perpendicular to  $F_x$  as shown in Figure 3 (b), and
- (2) the average of the unit normal vectors of the all the faces sharing  $\mathbf{p}_x$  and being exposed to the outside of the mesh, which gives an approximated normal vector of the target domain at  $\mathbf{p}_x$ , makes more than 90 degrees with the normal vector of  $F_x$ .



(a) A preliminary tetrahedral mesh



(b) A preliminary tetrahedral mesh  
(Cross section)

Figure 2 An example of the preliminary tetrahedral mesh

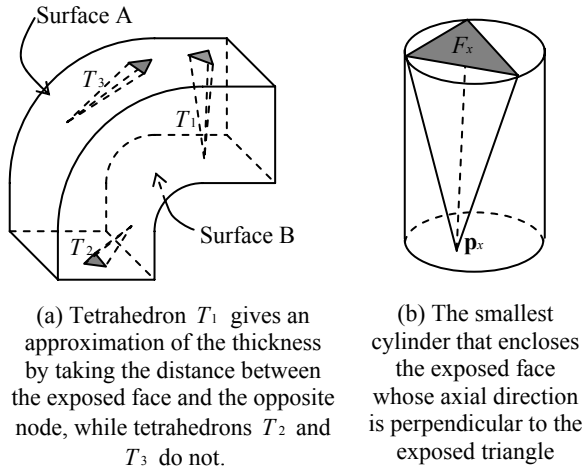


Figure 3 Typical configurations of a tetrahedron with only one face exposed to the outside of the mesh

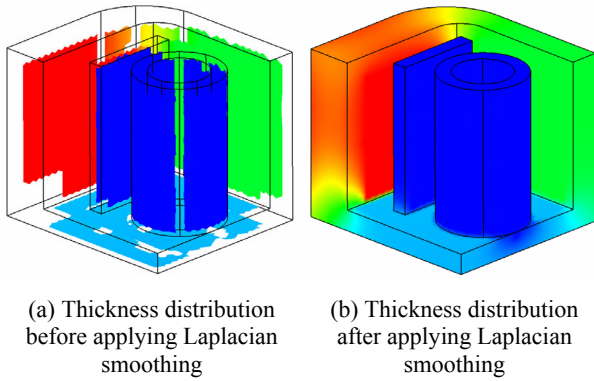


Figure 4 Thickness distribution

When some tetrahedrons sharing a node satisfy the above criteria, the proposed method assigns to that node the smallest approximated thickness among the thicknesses calculated from the tetrahedrons sharing the node.

It should be noted that the approximated thickness may not be assigned to a node if none of the tetrahedrons sharing the node satisfies the above criteria. For example, only nodes in the shaded area shown in Figure 4 (a) are assigned with an approximated thickness. For other nodes, the method calculates the approximated thickness by applying Laplacian smoothing. During this process, thicknesses that are already assigned are fixed, and an initial guess of the thickness (typically zero) is assigned to every node for which a thickness is not yet assigned. Each guess of the thickness is replaced in each iteration with the average of the thicknesses assigned to the neighbors that are connected to the node with one edge. The iterations continue until the maximum change in the estimated thickness is smaller than a given tolerance, typically  $10e-6$ . The thickness distribution after applying Laplacian smoothing is shown in Figure 4 (b).

After an approximated thickness is assigned to every node, the thickness distribution on the surface of the target geometric

domain,  $t(\mathbf{x})$ , can be calculated by interpolating the thickness values on the nodes.

#### 4 Creating a Single-Layer Tetrahedral Mesh

After calculating the thickness distribution  $t(\mathbf{x})$ , the method creates a surface triangular mesh with element sizes adapted to the thickness distribution; the triangles and nodes of the surface triangular mesh are then connected to create a single-layer tetrahedral mesh. The element sizes of the surface triangular mesh are adapted to the thickness distribution so that a triangle makes a near equilateral tetrahedron when it is connected to a node lying on the opposite surface. The height (the distance from a node to the opposite face) of an equilateral tetrahedron with edge length of 1.0 is  $\sqrt{2/3}$ . Hence, the edge length of an equilateral triangle located where the thickness is  $t$  must be  $t/\sqrt{2/3}$  to have a chance to become an equilateral tetrahedron when it is connected to a node lying on the opposite surface.

Anisotropy, as well as thickness, can be taken into account when computing the desired edge length of the surface triangles. In plastic injection molding simulation, an anisotropic mesh often gives a good result with fewer elements (i.e., less computational time). Elements can be stretched along the flow direction because the gradient of the physical quantities of the fluid is smaller along the flow direction compared to the gradient in the perpendicular direction of the flow. Since the flow direction of the fluid plastic injected to a thin-walled solid tends to be parallel to the wall of the solid, larger surface triangles yield such an anisotropic tetrahedral mesh. As a result, the sizing function that gives desired edge lengths over the surface of a target geometric domain can be written as  $s(\mathbf{x}) = ct(\mathbf{x})/\sqrt{2/3}$ , where  $c$  ( $c \geq 1$ ) is a stretching factor for an anisotropic mesh ( $c = 1$  yields an isotropic mesh).

The proposed method uses the bubble-packing method [Shimada and Gossard 1998; Shimada et al. 2000; Yamakawa and Shimada 2004] to create a surface triangular mesh that complies with the sizing function. The bubble-packing method packs bubbles on the surface of the target geometric domain to find good node locations, and the nodes are connected to create a triangular mesh. A single-layer tetrahedral mesh is then created from the surface triangular mesh by the Delaunay tetrahedralization technique using the triangular mesh as input.

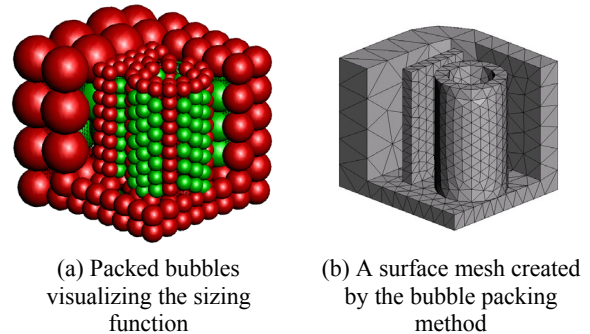


Figure 5 A surface triangular mesh created by the bubble packing method

The quality of the single-layer mesh is improved by applying a post-process called “local transformation” [Joe 1995]. The Delaunay tetrahedralization technique often creates low quality tetrahedrons known as slivers. The local transformation technique modifies the node connections near the low quality elements and effectively eliminates such slivers.

## 5 Subdividing Tetrahedrons into $n$ Layers

When multiple-layer tetrahedral mesh is needed, the method subdivides every tetrahedron into  $n$  layers after creating a single-layer mesh. For example, Figure 6 shows a three-layer mesh created by subdividing a single-layer mesh. To maintain the conformity of the mesh, each triangular face of a tetrahedron must be subdivided into the pattern that adds  $n-1$  nodes on each edge,

$\sum_{k=1}^{n-2} k$  nodes inside. The inside edges must be added so that the pattern does not change regardless the order of the three nodes of the triangle. For example Figure 7 (a) shows a subdivision pattern of a face when  $n=3$ . Although such a subdivision template is already well known, the orientation of the template must be carefully chosen to always produce  $n$  layers along the thickness direction; this section re-caps the construction of the template and discusses the orientation of the template.

The subdivision pattern of a tetrahedron is constructed as follows: Consider a tetrahedron with three edges lying on three orthogonal axes  $u$ ,  $v$  and  $w$  and the lengths of the three edges are  $n$  as shown in Figure 7 (b). The node at the origin is denoted as  $\mathbf{o}$ , and the other three nodes lying on axes  $u$ ,  $v$  and  $w$  are denoted as  $\mathbf{p}$ ,  $\mathbf{q}$ , and  $\mathbf{r}$  respectively. A cube is then created that shares the three edges of the tetrahedron  $\mathbf{o}-\mathbf{p}$ ,  $\mathbf{o}-\mathbf{q}$ , and  $\mathbf{o}-\mathbf{r}$ , and subdivides the cube into smaller sub-cubes in  $n \times n \times n$  grid pattern. Figure 8 (a) shows the sub-cubes intersecting with the plane  $u+v+w=n$ . Then each sub-cube is subdivided into two triangular prisms by a plane parallel to  $u+v=0$  as shown in Figure 8 (b); each prism is subdivided into one tetrahedron and one pyramid (a quadrilateral face and four triangular faces) by a plane parallel to  $u+v+w=0$  as shown in Figure 8 (c). The two pyramids are subdivided into four tetrahedrons by a plane parallel to  $u-w=0$  as shown in Figure 8 (d). The six tetrahedrons are finally created from a sub-cube as shown in Figure 8 (e), and  $6n^3$  tetrahedrons are created in total. All tetrahedrons that have at least one node not satisfying  $u+v+w \leq n$  are deleted to complete the subdivision template for a tetrahedron.

This subdivision template subdivides a tetrahedron into  $n^3$  tetrahedrons and always creates  $n$  layers between any node and its opposite face, across edges  $\mathbf{o}-\mathbf{r}$  and  $\mathbf{p}-\mathbf{q}$ , and across edges  $\mathbf{o}-\mathbf{p}$  and  $\mathbf{r}-\mathbf{q}$ . However, the template creates only  $n-1$  layers across edges  $\mathbf{o}-\mathbf{q}$  and  $\mathbf{r}-\mathbf{p}$  because the edge created for subdividing the two pyramids, which is a diagonal of the sub-cube (shown in Figure 8(c)), connects two nodes that must be two layers apart. This diagonal edge cuts across the layers only when layers are created across edges  $\mathbf{o}-\mathbf{q}$  and  $\mathbf{r}-\mathbf{p}$  (otherwise the edge lies on the interface between layers). Hence, when the subdivision template is applied to a tetrahedron with two opposing edges lying on the opposite surfaces of the solid, edges  $\mathbf{o}-\mathbf{q}$  and  $\mathbf{r}-\mathbf{p}$  must be mapped to the two edges connecting the opposite surfaces so that the subdivision template does not lose one layer across the surfaces.

## 6 Discussion

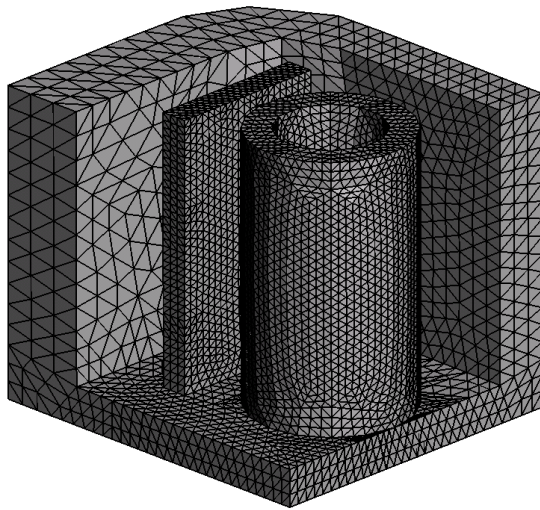
The method assumes that the input geometry is a thin-walled solid. If a chunky solid is given as input, thickness estimation may fail. For example, if a sphere is given as input, none of the tetrahedrons included in the preliminary tetrahedral mesh will satisfy the criteria for identifying the tetrahedron that can give an approximated thickness. Thus the input geometry must be mostly thin walled. However, this limitation does not impact the applicability of the method to the finite element analyses of plastic injection molding because virtually all the injection-molded plastic parts are thin-walled.

The method creates a specified number of layers as long as a thickness can be uniquely calculated. The method may fail to create a specified number of layers where the thickness is ambiguous. For example, when two plates of different thickness are connected, the thickness at the intersection is ambiguous, and thus the method may not create exactly a specified number of layers. Such irregularity, however, occurs in a limited region, and thus an effect of such irregularity on the accuracy of the analysis is insignificant.

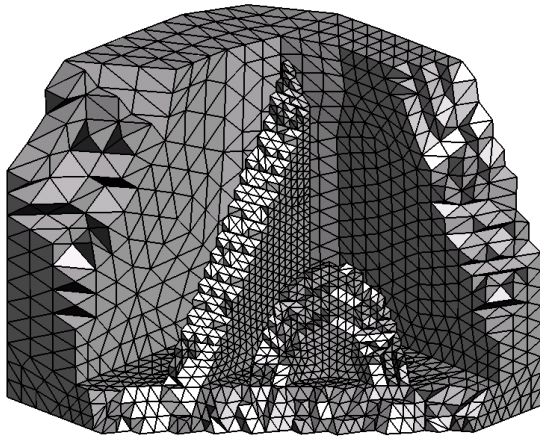
## 7 Layered Tet Mesh Examples

Some examples are presented in this section. Figure 9 shows single-layer and two-layer meshes of a cell phone case. Figure 9 (a) shows a single-layer mesh of the cell phone case, and the close up image of a cross section shows that the element sizes are successfully adapted to the thickness. The quality of the mesh is shown in Figure 9 (c) by radius ratio, which is the radius of the inscribed sphere divided by the radius of the circumscribed sphere. The radius ratio of an equilateral tetrahedron is 3.0; it increases as a tetrahedron becomes flatter. The histogram shown in Figure 9 (c) indicates that most tetrahedrons have a radius ratio close to 3.0, i.e., most tetrahedrons in the single-layer mesh are well shaped. Figure 9 (b) shows a two-layer mesh of the cell phone case created by applying the subdivision template to the mesh shown in Figure 9 (a). The close-up image of a cross section shows that the mesh is successfully subdivided into two layers. The quality of the two-layer mesh is shown in Figure 9 (d). The histogram shown in Figure 9 (d) indicates that most tetrahedrons have a radius ratio close to 3.0, and the overall quality is good. However, 3,716 tetrahedrons have a radius ratio of over 12.5, and the worst radius ratio is 295.16. Although the worst tetrahedron is very flat, such a tetrahedron can be accepted for a mold flow simulation when the tetrahedron lies along the flow direction, which in most cases is parallel to the interface between layers. None of the flat tetrahedrons included in the mesh cut across the layers because all the tetrahedrons are subdivided into two layers, and thus are most likely to lie along the flow direction.

The computational time for creating a layered mesh from a single-layer mesh is very small. It took 5.5 seconds to create the two-layer mesh shown in Figure 9 (b) from the single-layer mesh shown in Figure 9 (a). Hence, once a single-layer mesh is created, layered meshes can be created very efficiently with the proposed method.

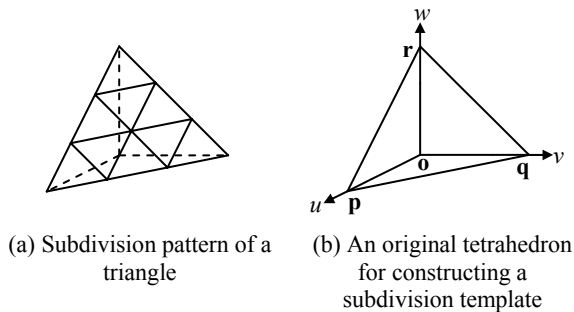


A three-layer mesh



A three-layer mesh (Cross section)

Figure 6 Example of a three-layer mesh



(a) Subdivision pattern of a triangle

(b) An original tetrahedron for constructing a subdivision template

Figure 7 Subdividing a tetrahedron into  $n$  layers

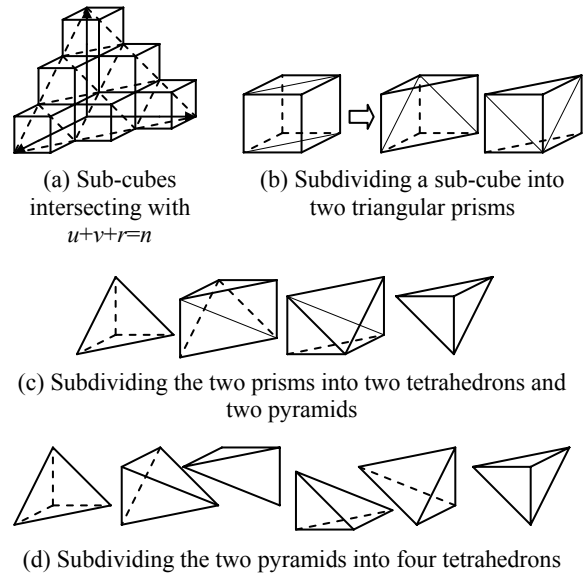


Figure 8 Constructing a subdivision template

## 8 Finite Element Analysis of Plastic Injection Molding

Plastic injection molding is used throughout industry to produce large quantities of inexpensive parts for a variety of uses. The injection molding process consists of two steps. First, molten plastic resin is injected under high pressure into a mold. The resin is then held in the mold until it has cooled sufficiently to be ejected. This process has several distinct advantages over other production methods, namely that complex parts can be produced quickly, reliably and with minimal overhead. Given the high demand for these plastic parts, design cycles must be as short as possible, with the minimum possible cost to the manufacturer.

Traditionally, the design of a new product involves iteration through several prototypes before settling on a final design. However, this process is very ill-suited to the design of injection molded plastic parts. This is due to the fact that the cost of creating a single mold for a new part could reach hundreds of thousands of dollars, though many plastic parts sell for less than a dollar apiece [Beaumont et al. 2002]. Furthermore, the mold for a particular piece must be as carefully designed as the product itself. A poorly designed mold could lead to air bubbles, structural weaknesses or any number of other problems in the final product—even if the mold cavity has the correct shape. The combination of these factors makes plastic injection molding a relatively high-risk venture to undertake.

In order to reduce the risk inherent to the injection molding process, finite element methods have been developed to predict the potential problems of a particular part before a mold is created. A well-designed finite element simulation should be able to predict the potential flaws in a part well before mold construction begins. Specialized finite element software is required for the analysis of injection molding, due to the complex nature of the injection process. This software works sequentially, mimicking the physical process of injection molding.

First, the software models the injection of resin into the mold. Potential filling problems, such as air traps and incomplete fills, can be identified in this step. Figure 10 (a) depicts a test mold

approximately half filled. Next, the packing and holding cycle is modeled. This is the stage of the process when the part remains in the mold and cools. By combining the results of these first two analyses, fiber orientation and warpage analyses can be conducted. Fiber orientation is of particular interest to parts whose structural properties are important. Many thermoplastics are mixed with tiny fibers before being injected. These fibers produce extra rigidity in the part, but this rigidity is strongly anisotropic. This is due to the fact that the fibers are long and thin, and only provide this additional rigidity along their length. Thus, knowing the fiber orientation after injection is crucial to knowing the structural properties of a part. The fiber orientation of a test part is shown in Figure 10 (b).

Warpage analysis is generally the final step in the analysis of an injection process. As the melt front moves through the mold, molten resin contacts the wall of the mold and immediately begins to cool and crystallize. Thus, the first resin to contact the wall is further along in the cooling process at the end of filling than the last resin to be injected. In addition, thicker portions of the mold cool slower than thinner portions. This difference in cooling time creates uneven volumetric contraction in the part, which leads to warpage. If the part is not properly designed, this warpage can exceed manufacturing tolerances, rendering the part useless. Thus, an accurate calculation of the total warpage of a part is extremely important for every injection molding simulation. The warpage of the test part, exaggerated by a factor of 5, is shown in Figure 10 (c).

The accuracy of a finite element solution depends strongly on the choice of mesh used in the analysis. A well-designed mesh will produce convergence towards a particular solution value as the number of elements increases. It is suggested that the layered tetrahedral meshes created by the proposed method will elicit these convergence trends in warpage simulations. To test this hypothesis, simulations are run on the test part using Timon3D [Toray Industries, Inc. 2002], a commercial software package for the analysis of injection molding. Simulations are run on a computer equipped with a 1 GHz Pentium III processor with 1 GB of RAM.

Three types of meshes are created for this analysis. The first is an unstructured tetrahedral mesh with no clear layer structure (see Figure 11 (a)). Two of these meshes are used, the first being a coarser mesh with 21,780 elements and the second being a finer mesh with 54,476 elements. The second type of mesh is a layered mesh consisting of largely isotropic tetrahedrons (see Figure 11 (b)). The third type is identical to the second, except that the tetrahedrons used are anisotropic, having edge length of 1.5 times the edge length of the isotropic mesh in the non-thickness dimension (see Figure 11 (c)). Meshes of these kinds having one through five layers are used in the analysis.

Default settings in Timon3D are used throughout the analysis with a few exceptions. First, injection points are chosen on the part. These are shown as blue arrows in Figure 12. While not typical of an actual mold, these three injection points are of particular geometric significance to the part. These points exist in all meshes, so simulations utilizing all three of the different types of meshes can use these same three points. Second, the resin is chosen because it has valid material data for use in all four types of analyses: filling, packing, fiber orientation and warpage.

Points on the part must be constrained in order to conduct a warpage analysis. These points are constrained in such a way as to model the part cooling and warping in free air, and also to

eliminate translation and rotation of the entire part. In order to accomplish both of these goals, the points are chosen as follows: First, an edge is chosen which contains the points of interest. This edge is shown in Figure 13. This edge, like the injection points, is chosen because it exists in all meshes. One of the end points of the edge is chosen to be constrained against translation in the x, y and z directions, while the other end is constrained such that it can only move in one direction. The x direction is chosen because the displacement between the first point and this point is primarily along the x direction. Finally, a third point — also of particular geometric significance — is chosen, and is constrained to move only in the plane defined by the three constrained points. These constraints can be seen as red arrows in Figure 12.

Injection, packing and warpage analyses are conducted using each mesh. Comparison of the different meshes is accomplished by comparing the total warpage of points along the edge shown in Figure 13 against their x coordinate. These results are summarized in Figure 14 (a), Figure 14 (b), and Figure 14 (c). Simulations of single-layer meshes are not included in these figures due to the fact that Timon3D analyzes such meshes as shell elements with a finite thickness. As can be seen in Figure 14 (b) and Figure 14 (c), the layered meshes show a clear convergence trend towards a particular solution as the number of layers increases. This supports the proposition that meshes composed of layered tetrahedral elements perform well in warpage analysis simulations of plastic injection molding.

Meshes with no clear layer structure do not exhibit this convergence trend (Figure 14 (a)). While not as conclusive, since only two simulations were run, it appears that the unstructured mesh is converging to a value substantially lower than the value predicted by the layered meshes, if it is converging towards anything at all. These results suggest that unlayered meshes are not appropriate for use in injection molding simulations. More simulations should be conducted to verify this claim.

The warpage results for the isotropic and anisotropic meshes differ by at most  $5 \cdot 10^{-2}$  mm when comparing simulations with the same number of layers. These results indicate a strong dependence of the solution on the number of layers and not necessarily on the number of elements. This is due to the fact that the volumes of individual elements in the anisotropic mesh are generally larger than those in the isotropic mesh. As such, the total number of elements in the anisotropic mesh is much smaller and simulation time is greatly reduced. The five-layer, isotropic simulation runs in approximately twenty-three hours, but only six hours are required for the five-layer simulation of the anisotropic mesh. These results strongly suggest that layered, isotropic, tetrahedral meshes are the better suited to injection molding simulations than the others tested.

## 9 Conclusion

A new method for creating a layered tetrahedral mesh of a thin-walled solid is presented. Such a mesh is particularly effective for obtaining an accurate result in finite element analysis of plastic injection molding. The method creates a preliminary tetrahedral mesh and estimates the thickness distribution over the surface of the target geometric domain. The method then calculates the ideal element size of the surface triangular mesh that yields well-shaped tetrahedrons when a triangle is connected to a node lying on the opposite surface from the estimated thickness distribution. The method creates a surface triangular mesh with size adapted to the ideal edge length and creates a single-layer mesh from the surface triangular mesh without inserting interior nodes. The single-layer

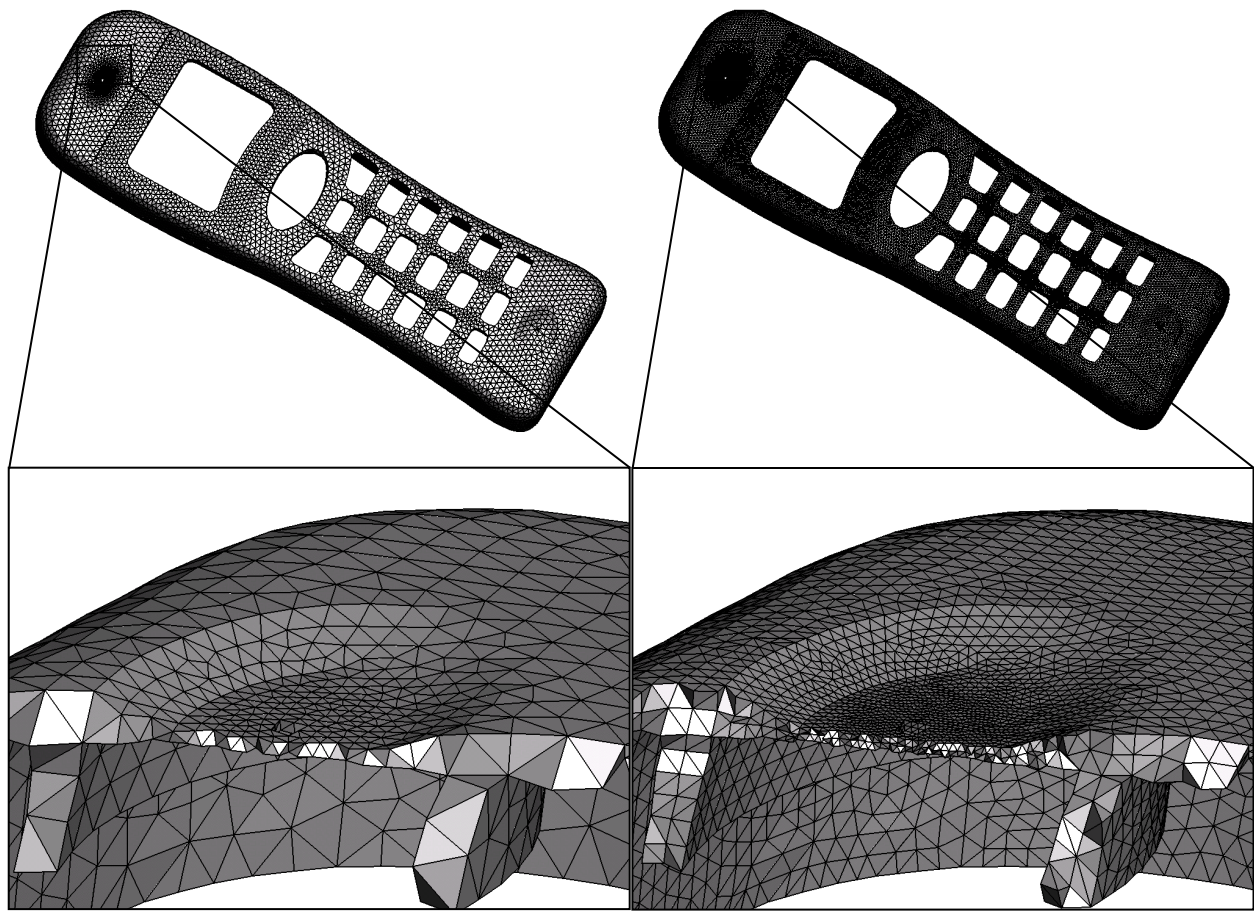
mesh is finally subdivided into  $n$  layers by applying a subdivision template. Some examples have been presented for showing that the method creates a good quality tetrahedral mesh.

The method is useful for injection molding simulation. The results of a series of finite element analyses using layered meshes created by the proposed method indicate that having more layers is more effective in improving the accuracy than uniformly increasing the mesh resolution. A more accurate solution can be obtained without significantly increasing the number of elements by using an anisotropic layered mesh.

## References

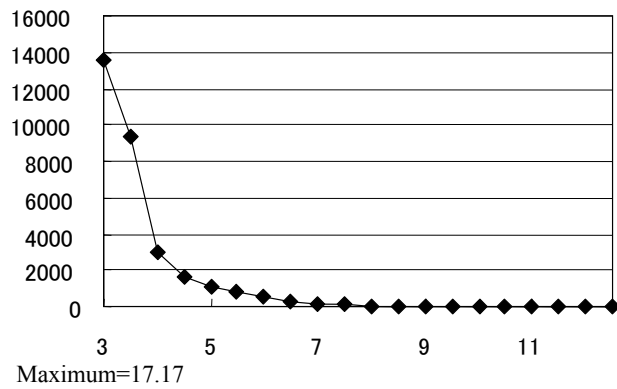
- Beaumont, J.P., Nagel, R., and Sherman, R. 2002. *Successful Injection Molding*. Hanser Gardner Publications Inc.
- Castro-Diaz, M.J., Hecht, F., and Mohammadi, B. 1995. New Progress in Anisotropic Grid Adaptation for Inviscid and Viscous Flows Simulations. In *Proceedings of 4th International Meshing Roundtable*, 73-85.
- Frey, P.J. and Alauzet, F. 2003. Anisotropic Mesh Adaptation for Transient Flows Simulations. In *Proceedings of 12th International Meshing Roundtable*, 335-348.
- Garimella, R.V. and Shephard, M.S. 2000. Boundary Layer Mesh Generation for Viscous Flow Simulations. *International Journal for Numerical Methods in Engineering* 49, 193-218.
- Garland, M. and Heckbert, P. 1997. Surface Simplification Using Quadric Error Metrics. In *Proceedings of ACM SIGGRAPH 97*, ACM Press / ACM SIGGRAPH, Computer Graphics Proceedings, Annual Conference Series, ACM, 209-216.
- George, P.L. 1999. Tet Meshing: Construction, Optimization and Adaptation. In *Proceedings of 8th International Meshing Roundtable*, 133-141.
- George, P.L., Hecht, F., and Saltel, E. 1991. Automatic Mesh Generator with Specified Boundary. *Computer Methods in Applied Mechanics and Engineering* 92, 269-288.
- Habashi, W.G., Dompierre, J., Bourgault, Y., Fortin, M., and Vallet, M.G. 1998. Certifiable Computational Fluid Dynamics Through Mesh Optimization. *AIAA Journal on Computational Fluid Dynamics Simulations* 36, 703-711.
- Joe, B. 1995. Construction of Three-Dimensional Improved-Quality Triangulations Using Local Transformations. *SIAM Journal on Scientific Computing* 16, 6, 1292-1307.
- Owen, S.J. and Saigal, S. 2000. Surface Mesh Sizing Control. *International Journal for Numerical Methods in Engineering* 47, 497-511.
- Peraire, J., Peiro, J., Formaggia, L., Morgan, K., and Zienkiewicz, O.C. 1988. Finite Element Euler Computations in Three Dimensions. *International Journal for Numerical Methods in Engineering* 26, 2135-2159.
- Peraire, J., Peiro, J., and Morgan, K. 1992. Adaptive Remeshing for Three-Dimensional Compressible Flow Computation. *Journal of Computational Physics* 103, 269-285.
- Peraire, J., Vahdati, M., Morgan, K., and Zienkiewicz, O.C. 1987. Adaptive Remeshing for Compressible Flow Computations. *Journal of Computational Physics* 72, 449-466.
- Persson, P.-O. 2004. PDE-Based Gradient Limiting for Mesh Size Functions. In *Proceedings of 13th International Meshing Roundtable*, 377-387.
- Quadros, W.R., Owen, S.J., Brewer, M., and Shimada, K. 2004. Finite Element Mesh Sizing for Surfaces Using Skeleton. In *Proceedings of 13th International Meshing Roundtable*, 389-400.
- Quadros, W.R. and Shimada, K. 2002. Hex-Layer: Layered All-Hex Mesh Generation on Thin Section Solids via Chordal Surface Transformation. In *Proceedings of 11th International Meshing Roundtable*, 169-180.
- Shewchuk, J. 2002. Constrained Delaunay Tetrahedralizations and Provably Good Boundary Recovery. In *Proceedings of 11th International Meshing Roundtable*, 193-204.
- Shimada, K. and Gossard, D.C. 1998. Automatic Triangular Mesh Generation of Trimmed Parametric Surfaces for Finite Element Analysis. *Computer Aided Geometric Design* 15, 3, 199-222.
- Shimada, K., Yamada, A., and Itoh, T. 2000. Anisotropic Triangulation of Parametric Surfaces via Close Packing of Ellipsoids. *International Journal of Computational Geometry and Applications* 10, 4, 417-440.
- Surazhsky, V., Alliez, P., and Gotsman, C. 2003. Isotropic Remeshing of Surfaces: A Local Parameterization Approach. In *Proceedings of 12th International Meshing Roundtable*, 215-224.
- Toray Industries, Inc. CAE - Software & Solution Business Department, *3D Timon Users Manual*, 2002
- Yamakawa, S. and Shimada, K. 2004. Triangular/Quadrilateral Remeshing of an Arbitrary Polygonal Surface via Packing Bubbles. In *Proceedings of Geometric Modeling and Processing 2004*, 153-162.
- Zienkiewicz, O.C. and Zhu, J.Z. 1991. Adaptivity and Mesh Generation. *International Journal for Numerical Methods in Engineering* 32, 783-810.



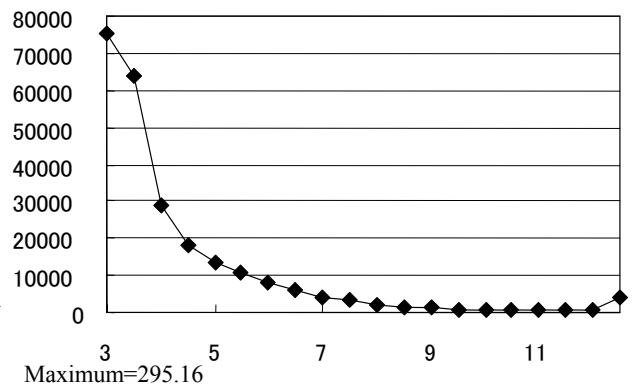


(a) Single-layer mesh of the cell phone case (10,872 nodes and 30,579 tetrahedrons)

(b) Two-layer mesh of the cell phone case (63,258 nodes and 244,632 tetrahedrons)

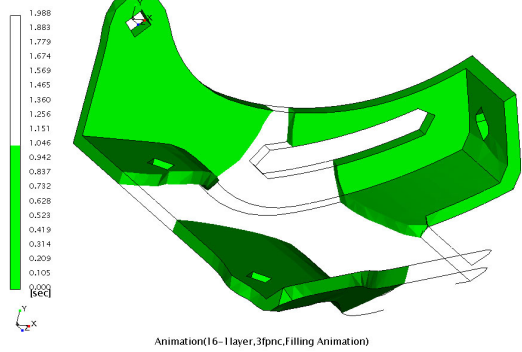


(c) Histogram and maximum of radius ratio of the single-layer mesh

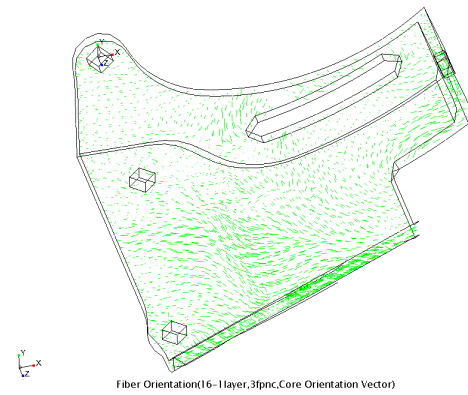


(d) Histogram and maximum of radius ratio of the two-layer mesh

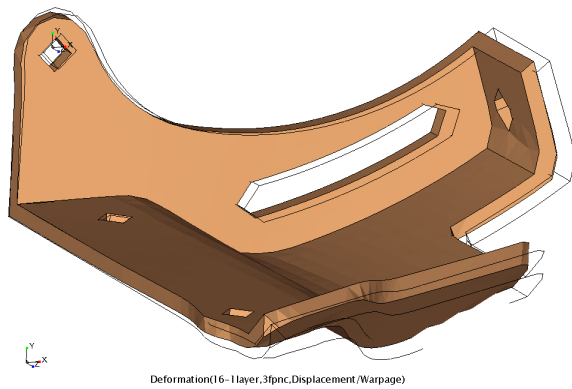
Figure 9 Layered meshes of a cell phone case



(a) Test mold approximately half filled

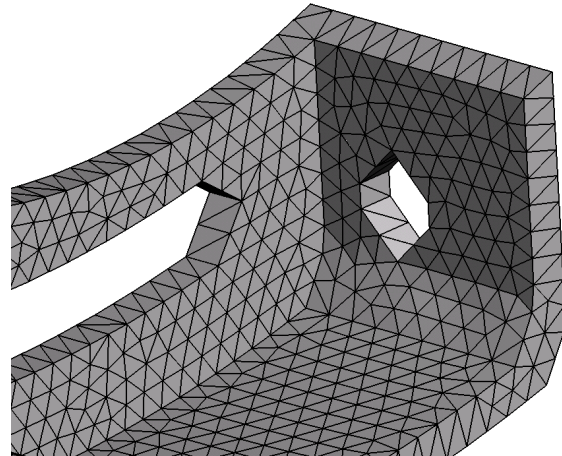


(b) Fiber orientation

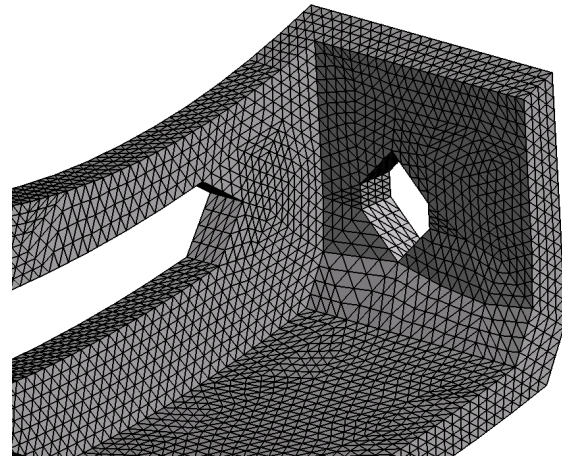


(c) Warpage exaggerated by a factor of 5

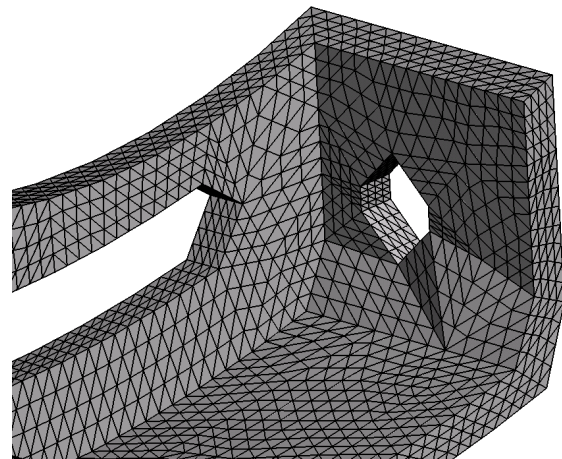
Figure 10 An example of injection molding simulation



(a) Unstructured mesh



(b) Isotropic layered mesh



(c) Anisotropic layered mesh

Figure 11 Three types of meshes used for the warpage analyses

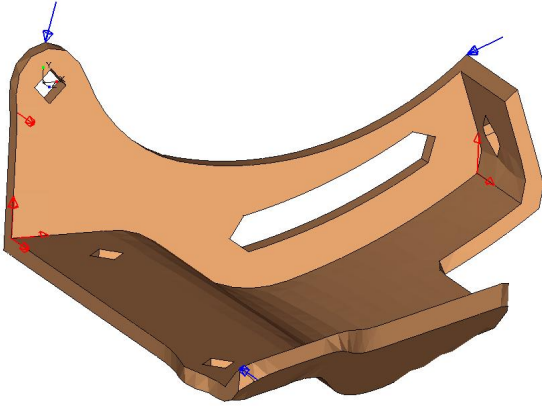


Figure 12 Boundary conditions for the warpage analyses

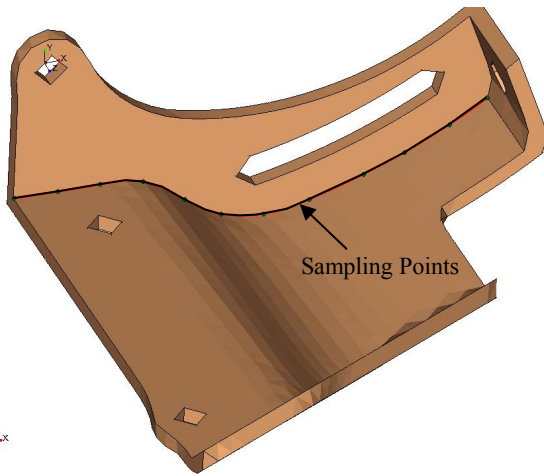
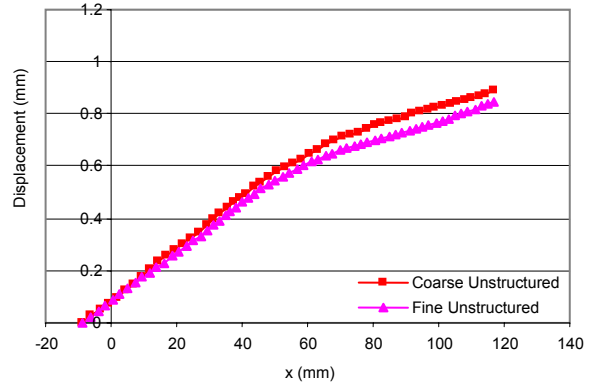
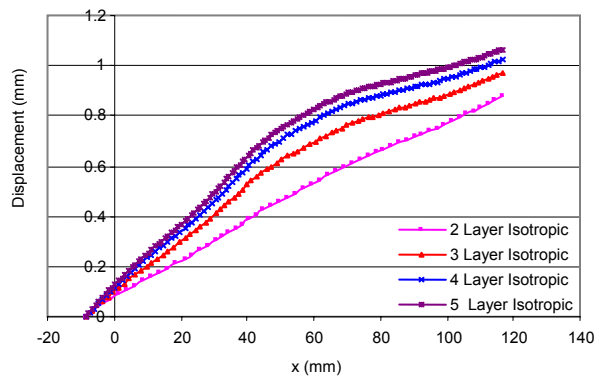


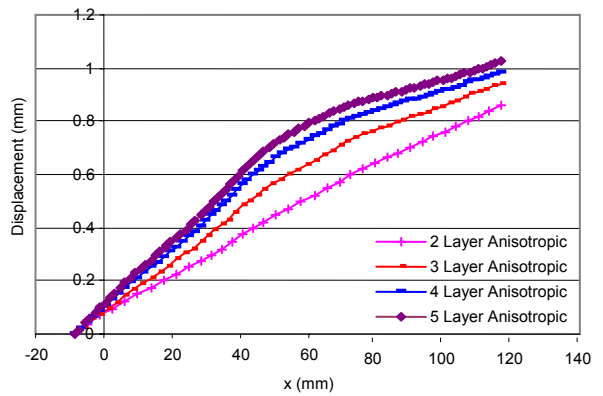
Figure 13 Sampling points for making the plots of the warpage analyses



(a) Unstructured meshes



(b) Isotropic layered meshes



(c) Anisotropic layered meshes

Figure 14 Results of the warpage analyses